AD

Technical Report ARAEW-TR-08013

DETERMINING THE TIME DEPENDENCE OF ELECTRICAL GRADIENTS IN RAILGUNS USING THE TRANSMISSION LINE MODEL

Mark A. Johnson
Paul J. Cote

September 2008

ARMAMENT RESEARCH, DEVELOPMENT AND ENGINEERING CENTER
Armaments Engineering & Technology Center
Weapon Systems & Technology
Benét Laboratories

Approved for public release; distribution is unlimited.

REPORT DOCUMENTATION PAGE	*Form Approved OMB No. 0704-0188*

1. REPORT DATE *(DD-MM-YYYY)*: xx-09-2008

2. REPORT TYPE: Final

3. DATES COVERED *(From - To)*: 2008

4. TITLE AND SUBTITLE

DETERMINING THE TIME DEPENDENCE OF ELECTRICAL GRADIENTS IN RAILGUNS USING THE TRANSMISSION LINE MODEL

5a. CONTRACT NUMBER

5b. GRANT NUMBER

5c. PROGRAM ELEMENT NUMBER

5d. PROJECT NUMBER

5e. TASK NUMBER

5f. WORK UNIT NUMBER

6. AUTHOR(S)

Johnson, Mark A. ; Cote, Paul J. *

7. PERFORMING ORGANIZATION NAME(S) AND ADDRESS(ES)

U.S. Army ARDEC, AETC
Benét Laboratories, AMSRD-AAR-AEW, B. 40
1 Buffington Street
Watervliet Arsenal, NY 12189-4000

8. PERFORMING ORGANIZATION REPORT NUMBER

ARAEW-TR-08013

9. SPONSORING/MONITORING AGENCY NAME(S) AND ADDRESS(ES)

U.S. Army ARDEC, AETC
Benét Laboratories, AMSRD-AAR-AEW, B. 40
1 Buffington Street
Watervliet Arsenal, NY 12189-4000

10. SPONSOR/MONITOR'S ACRONYM(S)

11. SPONSOR/MONITOR'S REPORT NUMBER(S)

12. DISTRIBUTION/AVAILABILITY STATEMENT

Approved for public release; distribution is unlimited.

13. SUPPLEMENTARY NOTES

*Battelle, Chapel Hill, NC 27517

14. ABSTRACT

A new technique has been developed for determining the time dependence of the inductance and resistance gradients of electromagnetic launchers. These are fundamental parameters when estimating launcher performance. The method is based on our analysis that shows how a transmission line model describes the relationship between the voltage gradient along the launcher rails and the rate of change of current. The approach extracts the gradients from experimental data by solving the normal equations associated with the transmission line model. An electromagnetic launcher was developed to test this new approach and experimental results are in excellent agreement with predicted behavior. This new technique provides a straightforward means to accurately determine the gradients of experimental designs under dynamic conditions. The data for these gradients are new and not available by any other known technique.

15. SUBJECT TERMS

Electromagnetic launchers, Resistance gradients, Inductance gradients

16. SECURITY CLASSIFICATION OF: a. REPORT	b. ABSTRACT	c. THIS PAGE	17. LIMITATION OF ABSTRACT	18. NUMBER OF PAGES	19a. NAME OF RESPONSIBLE PERSON
U/U	U	U	U	7	19b. TELEPHONE NUMBER *(Include area code)*

INSTRUCTIONS FOR COMPLETING SF 298

1. REPORT DATE. Full publication date, including day, month, if available. Must cite at least the year and be Year 2000 compliant, e.g. 30-06-1998; xx-06-1998; xx-xx-1998.

2. REPORT TYPE. State the type of report, such as final, technical, interim, memorandum, master's thesis, progress, quarterly, research, special, group study, etc.

3. DATES COVERED. Indicate the time during which the work was performed and the report was written, e.g., Jun 1997 - Jun 1998; 1-10 Jun 1996; May - Nov 1998; Nov 1998.

4. TITLE. Enter title and subtitle with volume number and part number, if applicable. On classified documents, enter the title classification in parentheses.

5a. CONTRACT NUMBER. Enter all contract numbers as they appear in the report, e.g. F33615-86-C-5169.

5b. GRANT NUMBER. Enter all grant numbers as they appear in the report, e.g. AFOSR-82-1234.

5c. PROGRAM ELEMENT NUMBER. Enter all program element numbers as they appear in the report, e.g. 61101A.

5d. PROJECT NUMBER. Enter all project numbers as they appear in the report, e.g. 1F665702D1257; ILIR.

5e. TASK NUMBER. Enter all task numbers as they appear in the report, e.g. 05; RF0330201; T4112.

5f. WORK UNIT NUMBER. Enter all work unit numbers as they appear in the report, e.g. 001; AFAPL30480105.

6. AUTHOR(S). Enter name(s) of person(s) responsible for writing the report, performing the research, or credited with the content of the report. The form of entry is the last name, first name, middle initial, and additional qualifiers separated by commas, e.g. Smith, Richard, J, Jr.

7. PERFORMING ORGANIZATION NAME(S) AND ADDRESS(ES). Self-explanatory.

8. PERFORMING ORGANIZATION REPORT NUMBER. Enter all unique alphanumeric report numbers assigned by the performing organization, e.g. BRL-1234; AFWL-TR-85-4017-Vol-21-PT-2.

9. SPONSORING/MONITORING AGENCY NAME(S) AND ADDRESS(ES). Enter the name and address of the organization(s) financially responsible for and monitoring the work.

10. SPONSOR/MONITOR'S ACRONYM(S). Enter, if available, e.g. BRL, ARDEC, NADC.

11. SPONSOR/MONITOR'S REPORT NUMBER(S). Enter report number as assigned by the sponsoring/ monitoring agency, if available, e.g. BRL-TR-829; -215.

12. DISTRIBUTION/AVAILABILITY STATEMENT. Use agency-mandated availability statements to indicate the public availability or distribution limitations of the report. If additional limitations/ restrictions or special markings are indicated, follow agency authorization procedures, e.g. RD/FRD, PROPIN, ITAR, etc. Include copyright information.

13. SUPPLEMENTARY NOTES. Enter information not included elsewhere such as: prepared in cooperation with; translation of; report supersedes; old edition number, etc.

14. ABSTRACT. A brief (approximately 200 words) factual summary of the most significant information.

15. SUBJECT TERMS. Key words or phrases identifying major concepts in the report.

16. SECURITY CLASSIFICATION. Enter security classification in accordance with security classification regulations, e.g. U, C, S, etc. If this form contains classified information, stamp classification level on the top and bottom of this page.

17. LIMITATION OF ABSTRACT. This block must be completed to assign a distribution limitation to the abstract. Enter UU (Unclassified Unlimited) or SAR (Same as Report). An entry in this block is necessary if the abstract is to be limited.

DETERMINING THE TIME DEPENDENCE OF ELECTRICAL GRADIENTS IN RAILGUNS USING THE TRANSMISSION LINE MODEL

Mark A. Johnson
Benet Laboratories
Watervliet Arsenal, NY 12189

Paul J. Cote
Battelle
Chapel Hill, NC 27517

ABTRACT

A new technique has been developed for determining the time dependence of the inductance and resistance gradients of electromagnetic launchers. These are fundamental parameters when estimating launcher performance. The method is based on our analysis that shows how a transmission line model describes the relationship between the voltage gradient along the launcher rails and the rate of change of current. The approach extracts the gradients from experimental data by solving the normal equations associated with the transmission line model. An electromagnetic launcher was developed to test this new approach and experimental results are in excellent agreement with predicted behavior. This new technique provides a straightforward means to accurately determine the gradients of experimental designs under dynamic conditions. The data for these gradients are new and not available by any other known technique.

1. INTRODUCTION

There are a number of electromagnetic (EM) propulsion technologies including rail, coil, and reconnection launchers (Ying, et al., 2004). Most current research efforts are focused on the rail launcher, or railgun. The simple railgun is comprised of 2 stationary parallel conductors (rails) and a moving armature. Current flows through the rails and armature producing a magnetic field between the rails which drives the components apart. Supporting structures keep the rails fixed while the armature is free to accelerate. The force between 2 coaxial current loops is proportional to the product of their currents and the inductance gradient as one loop moves (Kolm, H. and Mongeau, P. 1984). The EM launchers envisioned for use in future military systems require energies that result in damage to both the conducting rails and insulating materials. The U.S. Army Armament Research, Development, and Engineering Center's Benet Laboratories is developing new technologies to enhance the bore life of railguns so that a viable system can be successfully fielded. We have developed new concepts on the origins of bore damage which explain how induced magnetic fields play a dominant role in these effects. Our results offer explanations for the erosion phenomena commonly observed in EM launcher firing tests and make it possible to design a system that mitigates the damage. We use the transmission line model to relate the distribution of voltages along the rails of a launcher to the rate of change of current. The transmission line model is the basis for obtaining the time dependence of the electrical gradients of EM launchers under typical firing scenarios. The resistance gradient (R_X) and inductance gradient (L_X) are critical to the operation of railguns. They directly relate to the force on the projectile and their time dependence has not previously been determined.

2. TRANSMISSION LINE MODEL

Fig. 1 shows a schematic of a simple railgun. The two parallel rails are separated by a distance h, with current, i, flowing towards the armature in the upper rail and flowing back from the armature in the lower rail. The magnetic field B is generated within the rails behind the armature which has accelerated the armature to velocity v. When there is no armature motion, the voltage distribution for the railgun in Fig. 1 is given by (Cote, 2007):

$$V(x,t) = V_B(t) - L_X(t) x di/dt - 2R_X(t) x i(t) \tag{1}$$

where $V_B(t)$ is the breech voltage, $L_X(t)$ is the distributed inductance of the rail, $R_X(t)$ is the distributed resistance, $V(x,t)$ is the rail-to-rail potential at a distance x from the breech, and $i(t)$ is the current.

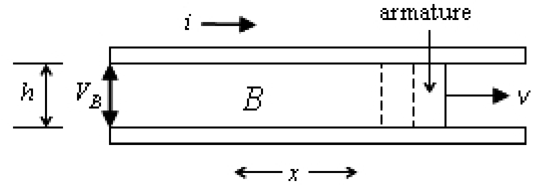

Fig.1. Schematic of a simple railgun.

Eq.(1) shows that for positive *di/dt*, the total voltage along the rail will be reduced below that impressed at the breech by the power supply and that reduction varies linearly with *x*. At negative *di/dt*, the total voltage along the rail will increase linearly with *x* along the rails. The total rail-to-rail voltage can exceed the breech voltage everywhere along *x* if the inductance term exceeds the resistance term. Taking the derivative of both sides of Eq. (1) gives:

$$\partial V(x,t)/\partial x = -L_X(t)di(t)/dt - 2R_X(t)i(t) \qquad (2)$$

This is similar to the familiar transmission line equation (Feynman, et al, 1964) relating the gradient of the voltage along a transmission line to the rate of change of current. Under static conditions (fixed armature position), Eq. (2) applies to the railgun. The linear dependences in rail-to-rail voltages along the rails, as described by Eqs. (1) - (2) are due to the uniform changes in flux throughout the volume. The gradients can be determined by solving the normal equations for the 2 parameter model of Eq. (2):

$$\begin{bmatrix} \sum\left(\frac{di}{dt}\right)^2 & \sum\frac{di}{dt}*i \\ \sum\frac{di}{dt}*i & \sum i^2 \end{bmatrix} * \begin{bmatrix} L_X(t) \\ R_X(t) \end{bmatrix} = \begin{bmatrix} -\sum\frac{\partial V}{\partial x}*\frac{di}{dt} \\ -\sum\frac{\partial V}{\partial x}*i \end{bmatrix} \qquad (3)$$

3. PROCEDURE

A small scale launcher was used to validate the transmission line model and extract the gradients in Eq. (3). Fig. 2 shows the pulsed power supply and Fig. 3 shows the corresponding launcher. Power is supplied by switched capacitive energy sources, each coupled with a pulse shaping and current limiting inductance. It is comprised of 4 banks of 20, 3500 μF electrolytic capacitors, with each bank coupled to a 10 μH inductor. The maximum available energy is 28 kJ. Pickup coils located at the center of each inductor provide a means of measuring the current based on mutual inductance with surrounding coil. The staging sequence is optimized to minimize pickup from the inductors of the other banks. The launcher shown in Fig. 3 is based on a design provided by the Institute of Advanced Technology in Austin, TX. It is 1m long with a 1.3 cm by 2.5 cm rectangular bore that uses replaceable rail liners and G10 insulators.

Tests were conducted at 100 V using all 4 capacitor banks (1.4 kJ) staged at 1.0 and 0.5 ms to simulate different current profiles. The lower energy minimized strain on the components. A 40 μΩ shunt was used at the muzzle to simulate a fixed armature to eliminate contributions associated with motional electromotive forces. Voltage data was collected at the breech and down bore locations 0.1, 0.4, 0.7, and 1 m using welded copper leads on rail liners inserted into the bore. The total current was recorded for each test. Two tests were conducted for each staging sequence and an average of the voltages and currents were used in the analysis.

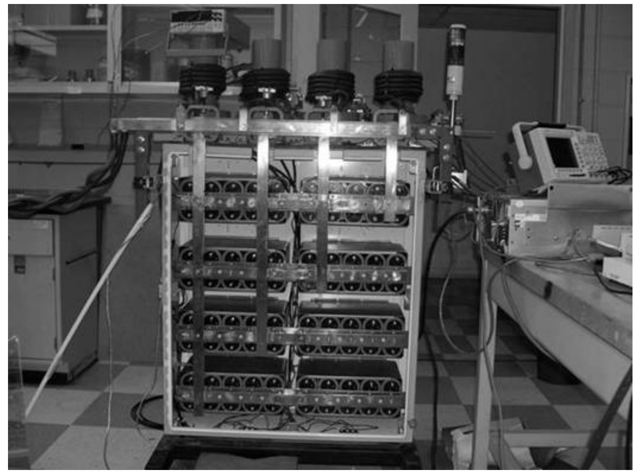

Fig 2. 28 kJ Pulsed power supply.

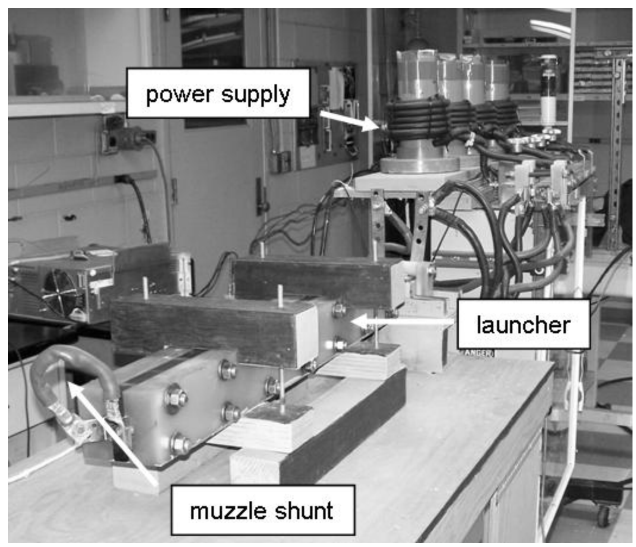

Fig 3. Small scale launcher based on design provided by the Institute of Advanced Technology in Austin, TX.

Fig. 4 shows $v(x,t)$ (x= 0.1, 0.2, 0.7, 1.0 m) for the 0.5 ms staging. Fig. 5 shows only $v(0.1,t)$ and $v(1.0,t)$, but with the current trace ($i(t)$) superimposed. The results are clearly consistent with the circuit description given by Eq. (2). At +*di/dt* , the rail-to-rail potential is reduced below the power supply potential (V_B) everywhere along the rails. At *-di/dt,* the rail-to-rail potential is actually higher than the power supply potential everywhere. The effect is the same for the 1.0 ms staging and has been observed to be even more dramatic with a greater *di/dt* obtained at higher energies using shorter staging (0.1 ms) times.

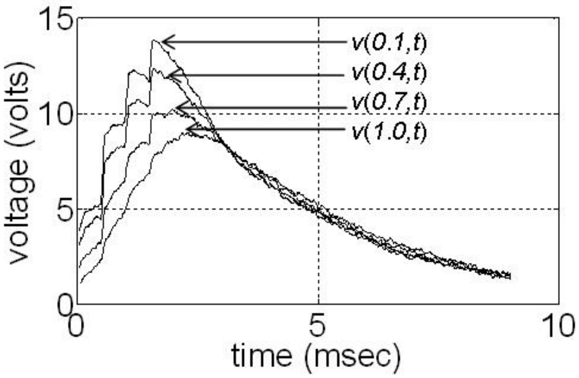

Fig.4. Rail-to-rail voltages measured at 4 positions relative to the breech for 0.5 ms staging.

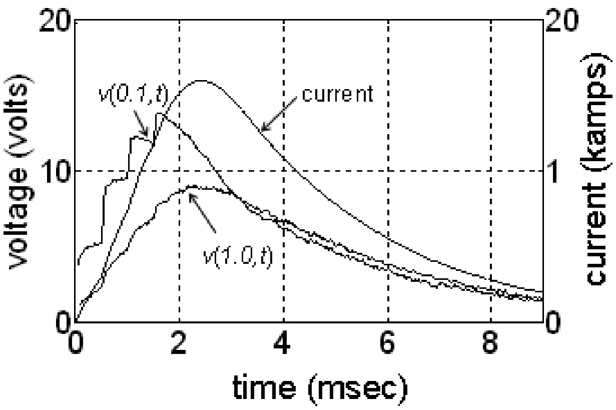

Fig. 5. Rail-to-rail voltages at breech and muzzle with current trace superimposed. Data is shown for 0.5 ms staging..

3. RESULTS

Figs. 6 and 7 show a comparison of $\partial V(x,t)/\partial x$ and $-L_X di/dt-2R_X\, i(t)$ using L_X and R_X obtained by solving the normal equations. The sharp peaks are a result of each of the 4 capacitor banks discharging at the appropriate time interval. All data points are used in the fit and the adjusted r^2 correlations of 0.95 and 0.97 demonstrates the validity of the model. The measured values of L_X = 0.56 μH/m for the 1.0 and 0.5 ms data and R_X = 75 μΩ/m (0.5 ms staging) and 73 μΩ/m (1.0 ms staging) are consistent and compare well with the theoretical estimates of L_X = 0.50 μH/m (Kerrisk, J.F, 1981) and R_X =70 μΩ/m.

The time dependence of the gradients was determined by solving the normal equations for the gradients using a subset of the data offset by discrete increments of time (sliding window). Data where field approached 0 was ignored since data in this region was dominated by noise. This eliminated data beyond 3.0 ms for the 0.5 ms tests and 4.0 ms for the 1.0 ms tests. The window used to compute the gradients was approximately 1 ms. The mean values of the gradients measured in these windows was determined to be L_X = 0.52 μH/m, R_X = 84 μΩ/m (0.5 ms staging) and L_X = 0.55 μH/m, R_X = 80 μΩ/m (1.0 ms staging). The results are consistent and L_X is in better agreement with predications than when all data is used in the estimates. This is likely a result of eliminating noisy data where the field approaches 0. The larger value of R_X is due to the skin effect.

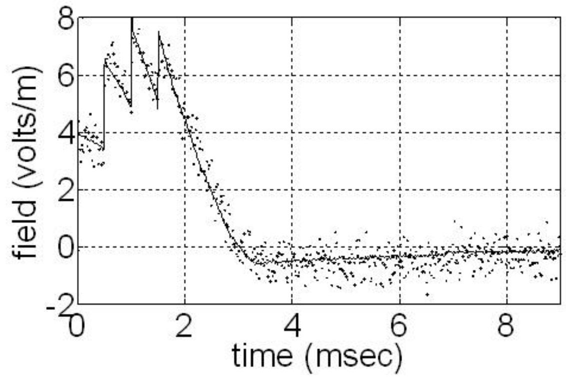

Fig. 6. Theoretical (solid line) and measured (points) rail-to-rail field values using 0.5 ms staging.
R_X = 75 μΩ/m L_X = 0.56 μH/m, and r^2 = 0.97.

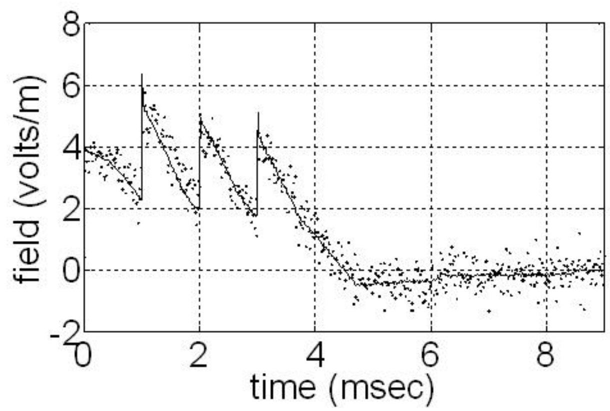

Fig. 7. Theoretical (solid line) and measured (points) rail-to-rail field values using 1.0 ms staging.
R_X = 73 μΩ/m L_X = 0.56 μH/m, and r^2 = 0.95.

Fig. 8 shows the normalized absolute deviation of the gradients from the mean values for the 0.5 ms tests. Results are similar for the 1 ms data. The figure shows that R_X is a strong function of time (skin effect) while L_X is relatively insensitive to time. We attribute this to fundamental differences in the physics of the two processes. The *IR* voltages are a function of the integrated currents in the rails while the instantaneous changes in current associated with the *Ldi/dt* voltages tend to be a surface phenomenon. The force on the armature is directly proportional to $L_X(t)$ so these results demonstrate that there is no change in the force due to the effects of current diffusion.

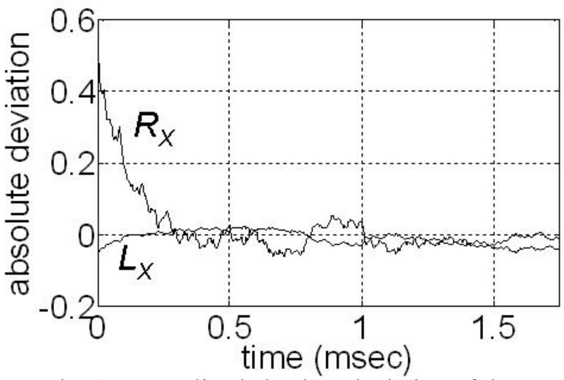

Fig. 8. Normalized absolute deviation of the gradients from the mean for 0.5 ms staging.

4. CURRENT DIFFUSION

In an effort to further validate the transmission line model of railgun fields, current diffusion into the rails was modeled to determine the effect of skin depth on our estimates. We assumed the depth of current penetration was proportional to the diffusion of a magnetic field into a conducting half-space for each rail. Given $i(t)$ at the boundary, the solution is given as (Knoepfel, H.E. 1970):

$$i_z(x,t) = \frac{2}{\sqrt{\pi}}\int_0^\infty i_0\left(t-\frac{1}{4\kappa_0}\frac{x^2}{\lambda^2}\right)e^{-\lambda^2}\,d\lambda \qquad (4)$$

This is a stationary solution for the depth of penetration x into the conductor assuming $i(t)$ is known at the boundary. We assumed a transient boundary condition $i_z(0,t) = 0$ for $-\infty < t < 0$ and $i_z(0,t) = i_0(t)$ for $0 \le t < \infty$. Assuming $i_z(x,0)=0$ for $0 < x < \infty$, the integration limits of the solution change to:

$$i_z(x,t) = \frac{2}{\sqrt{\pi}}\int_{x/2\sqrt{\kappa_0 t}}^\infty i_0\left(t-\frac{1}{4\kappa_0}\frac{x^2}{\lambda^2}\right)e^{-\lambda^2}\,d\lambda \qquad (5)$$

We modeled the rail as an infinitely long rectangular (0.32 x 0.008 m) copper conductor with a 260 μm^2 cross sectional area. The rail cross section was divided into 30 equal segments, each with an R_X of 2.3 mΩ/m. The estimate of $R_X(t)$ was determined by the area consumed by the measured current that diffused into the segments normalized by the peak current in the segments. Fig. 9 illustrates the diffusion of the measured current into the rail for the 0.5 ms staging. Results are consistent with COMSOL Multiphysics (COMSOL, AB) models of current diffusion into a bulk conductor. Fig. 9 also shows the effect of the integrated currents associated with the *IR* voltages and the surface phenomenon related to *Ldi/dt*.

Fig. 10 shows a comparison of the predicted and measured values of $R_X(t)$ for 0.5 ms staging. Results for the 1.0 ms staging were similar. The measured $R_X(t)$ were obtained directly from Eq. (2) using a 45 μs window and L_X fixed at 0.52 μH/m. The assumption of a fixed L_X was based on results shown in Fig 8. This eliminated the numerical inaccuracies associated with solving the normal equations to obtain both $L_X(t)$ and $R_X(t)$ with limited data (10 points) in the 45 μsec window. The results are in excellent agreement with theoretical predications.

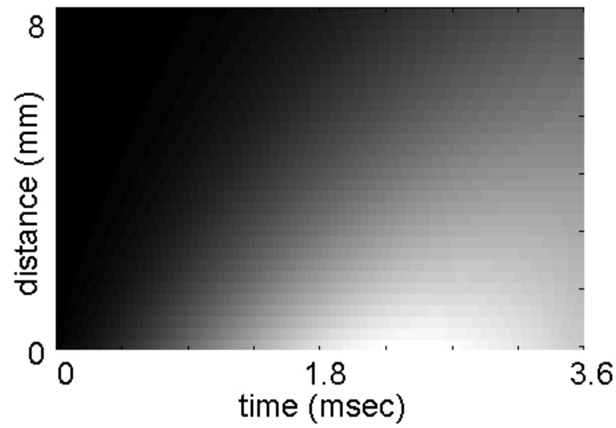

Fig. 9. Diffusion of current into rail for 0.5 ms staging. Brightness corresponds to current intensity.

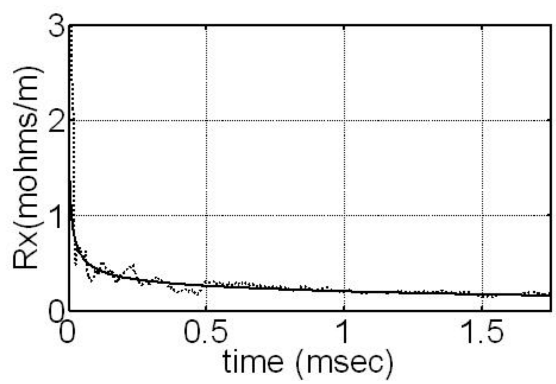

Fig. 10. Comparison of predicted (solid line) and measured (points) $R_X(t)$ for 0.5 ms staging.

5. SUMMARY

We are developing new technologies to enhance the bore life of railguns and have developed new concepts on how induced magnetic fields play a dominant role in bore damage. We use the transmission line model to relate the distribution of voltages along the rails of a launcher to the rate of change of current. This model provides the basis for obtaining the time dependence of the electrical gradients of EM launchers under typical firing scenarios. The resistance gradient (R_X) and inductance gradient (L_X) are critical to the operation of railguns. They directly relate to the force on the projectile and their time dependence has not previously been determined. This method determines $R_X(t)$ and $L_X(t)$ using experimental measurements under simulated firing conditions. We tested this approach using an experimental launcher operating under different firing scenarios and obtained consistent results that are in excellent agreement with theoretical predications. We have shown changes in $R_X(t)$ due to the skin effect and determined that current diffusion has little, if any, affect on L_X . The data for $R_X(t)$ and $L_X(t)$ are new and not available by any other known technique.

REFERENCES

COMSOL is a registered trademark of COMSOL AB

Cote, P.J, Johnson, M.A., Truszkowska, K., and Vottis, P. 2007: On the Role of Induced Fields in Railguns, *J.Phys. D*: *Appl. Phys*., **40,** 274-283.

Feynman, R., Leighton, R., and Sands, M. 1964: *The Feynman Lectures in Physics vol II*, 3rd ed. Addison Wesley, 238 pp.

Kerrisk, J.F., 1981: Current Distribution and Inductance Calculations for Rail Conductors, Los Alamos National Laboratory Tech. Rep. LA-9092-MS. 18 pp.

Knoepfel, H.E. 1970: *Pulsed High Magnetic Fields: Physical Effects and Generation Methods Concerning Pulsed Fields Up to the Megaoersted Level.* 1st ed. American Elsevier Publishing Company. 372 pp.

Kolm, H. and Mongeau, P. 1984: Basic Principles of Coaxial Launch Technology, *IEEE Transactions on Magnetics*, **20**, No.2, 227-230.

Ying, w., Marshall, R., and Shukang, C. 2004: *Physics of Electric Launch*. 1st ed. Science Press, Beijing. 450 pp.